Materials Research Proceedings 28 (2023) 1091-1100 https://doi.org/10.21741/9781644902479-120

FSW process mechanics and resulting properties for dissimilar Al-Ti T-joints

RANA Harikrishna [1,a*], BUFFA Gianluca [1,b], FRATINI Livan [1,c]

[1]Department of Engineering, University of Palermo, Viale Delle Scienze, 90128 Palermo, Italy

[a]hairkrishnasinh.rana@unipa.it, [b]gianluca.buffa@unipa.it, [c]livan.fratini@unipa.it

Keywords: FSW, T-Joint, Dissimilar, Skin, Stringer, Titanium, Aluminum, Material Flow

Abstract. Emergent manufacturing demands for superior performance but lightweight structures have pinpointed the development of multi-material and hybrid structures specifically in the aerospace and automotive industrial sectors. Friction stir welding (FSW), a solid-state joining technique has been proven very effective to produce joints between materials possessing extremely diverse thermal and mechanical properties. The present research aims to investigate the feasibility of Al-Ti skin-stringer joints with different plate geometries and placements. The effect of different approaches on material flow, grain morphology, intermittent phases, joint resistance, and microhardness are discussed in depth.

Introduction

Multi-material components are enticing recognition for their unique application base catering to automotive, aerospace, and transportation industries. Multi-material components not only present the unique benefits of demonstrating the properties of the individual materials but their advantages as a union too. The joining between titanium(Ti) and aluminum(Al) can be proposed for numerous applications in aeronautic and automotive sectors, wherein the higher strength-to-weight ratio is crucial in terms of body weight reduction and fuel savings. Conventional thermo-fusion joining techniques struggle with metallurgical challenges owing to a substantial disparity in physical properties, inadequate mutual solubility, and formation of brittle intermetallics (IMCs) [1,2].

The solid-state welding process was adopted into Al-Ti dissimilar joining and had been proven to be an efficacious technology by a few works of literature [3,4]. However, the formation of brittle IMCs like $TiAl_3$, $TiAl_2$, TiAl, Ti_3Al, Ti_2Al_5, $TiAl_2$, and Ti_2Al_5 was difficult to control during the welding. Alternatively, FSW has been proven to be an efficient process to eradicate the formation of IMCs up to a certain extent as compared to other solid-state welding processes [3,5,6]. This technique has been efficient to produce extremely arduous dissimilar welding joints owing to its less heat input feature. Moreover, with an innovative approach to in-process cooling Patel et al. [3] have reported a considerable decrease in the quantity of IMCs, which increased joint efficiency. To date, numerous investigations featuring butt and lap configuration joints with different process parameters have been reported [7-9]. According to these studies, the IMC layer thickness can be downed up to 2µm with a proper set of FSW parameters. Moreover, from the literature mentioned, the ideal range for revolutionary pitch (RP) during FSW with butt configuration joints was 0.05-0.10 which delivered 80-110% joint efficiency [7,9,10]. Apart from common process parameters like tool rotation speed (TRS), tool traverse speed (TTS), tool tilt angle, etc. Li et al.[8] experimented with the tool offset and reported the turbulent material flow in the nugget zone (NZ) during FSW with an increase in tool offset and a decrease in RP. However, vortex material flow is desirable during FSW as it distributes the fine Ti particle in Al substrates and makes a uniform composite structure delivering enhanced properties[3]. A few investigations have reported the reduction in the IMCs by using a thin interlayer during the FSW of Al-Ti butt configuration joints. The interlayer alloy having the higher affinity to the substrate withholds the formation of brittle IMCs, ensuing enhanced properties of the prepared joints [11]. Yet, Al-Ti "T" configuration joints produced by FSW have not been reported in the literature (except one reported by own research group) as per author's best knowledge owing to the complexities involved.

The literature survey discussed to the point indicates a lack of literature available in the field of Al-Ti "T" configuration FSW joints despite having a huge potential and promising sectors to explore. The objective of the present investigation is to produce successful Al-Ti "T" configuration FSW joints experimenting with parameters including substrate plate position swap and geometrical features. The influence of these variables on the mechanical and microstructural features like joint strength, microhardness, and IMCs distribution is studied in detail. This investigation is an extension of the work carried out by authors elaborating on the influences of several FSW parameters like TRS, TTS, and material positioning as skin/stringer[12].

Materials and Procedure

Materials and Process.

Substrates of aluminum alloy 6156 (Si 1 wt.%, Mg 0.9 wt.%, Cu 0.9 wt.%, Fe 0.1 wt.%, Mn 0.55 wt.%, Cr 0.125 wt.%, Zn 0.4 wt.%, Al – bal) and commercially pure titanium grade 2 with plate dimensions 140 × 90 × 3 mm and 140 × 90 × 2 mm respectively were used for experiments. A fully automatic FSW machine (Make: ESAB, Model: LEGIO 3ST) was used for conducting the experiments. An experimental setup with fixture and tool is displayed in Fig.s 1(a) and (b). Each experiment was conducted with position control mode and using a push roller on the leading edge of the Tungsten-Rhenium conical tool to ensure uniform contact conditions and plunge. TRS and TTS were chosen from the best welding conditions derived from the authors' recent publication [12]. The experiments were repeated thrice with each processing condition to ensure the credibility of the results. To understand the effect of slots in the skin, specimens were prepared with three different slot depths of 0 mm, 0.5mm and 1 mm longitudinally. Table 1 summarises each parametric condition with its unique experiment ID.

Table 1. Parametric sets with relative specimen IDs.

Specimen ID	**A**	**B**	**C**	**D**	**E**	**F**	**G**	**H**	**I**
Skin Material	**Titanium Grade 2**			**Al 6156**					
Skin Slot Depth [mm]	**0**	**0.5**	**1**	**0**	**0.5**	**1**	**0**	**0.5**	**1**
Tool Feed, F [mm min^{-1}]	40			50			70		
Tool Rotation Speed [rev. min^{-1}]	400			800			1000		
Tool Tilt Angle	2.5°								

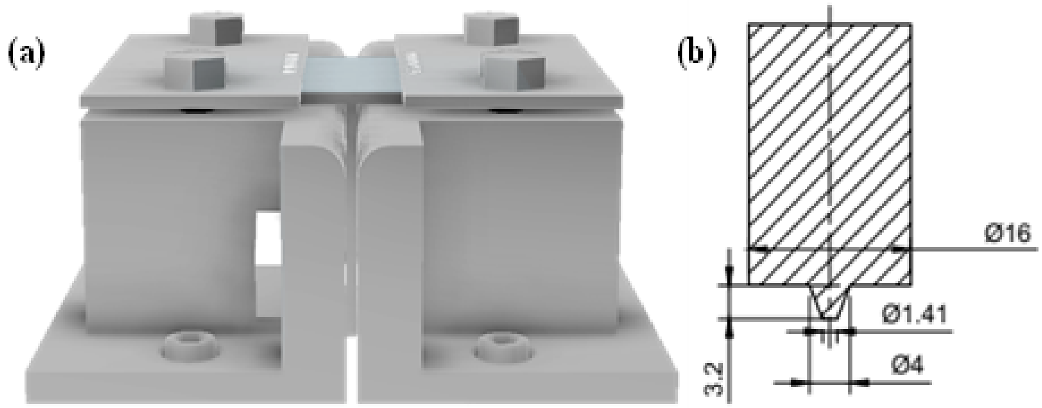

Fig. 1. Experimental setup (a) T-joint custom-designed fixture (b) WC-Re FSW tool geometry.

Microstructural Characterization

The specimens for microstructural examinations were obtained by sectioning at the center of the weld. They were further mounted, ground, and polished finally with 0.5µm diamond paste. Each joint specimen was etched with Keller's reagent (HF 2% vol. + HCL 3% vol. + HNO_3 5% vol. + H_2O 90% vol.) for the AA 6156 section and Kroll's reagent (HF 3% vol. + HNO_3 5% vol. + H_2O 90% vol.) for Ti Grade 2 section. Further, microstructural characterization was carried out through optical microscopy (OM) (OLYMPUS, Model-Inverted Metallurgical Microscope GX51), scanning electron microscopy (SEM), and energy dispersive spectroscopy (EDS) (Make: Zeiss, Model: Ultra-55 SEM).

Hardness and Tensile Testing

Each joint specimen was examined for microhardness using Eseway 4302 Vickers hardness tester (according to ASTM E-384). A square-based pyramid diamond indenter (136° intersects) was employed for tests with load and dwell time of 5 kg and 15 seconds, respectively. A specially designed fixture as displayed in Fig. 2 was used for conducting T- pull tests on a conventional tensile testing machine with a velocity of 2 mm/minute. The fractured specimens were further examined by SEM fractographic analysis.

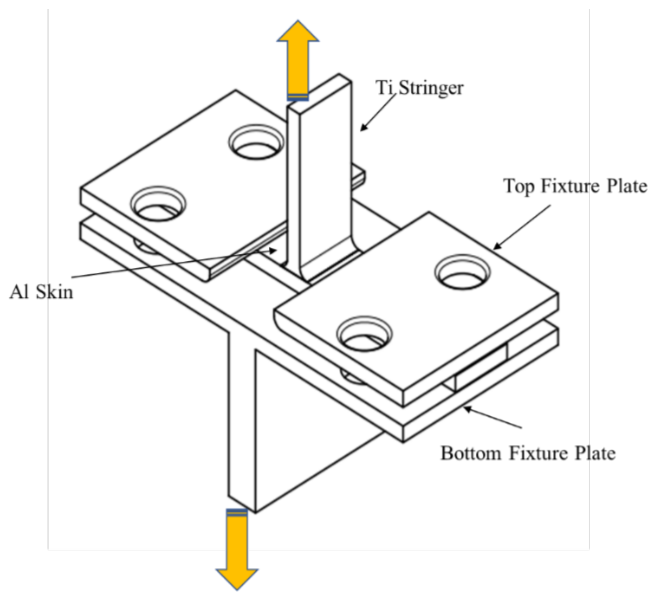

Fig. 2. Schematic of T-pull test fixture.

Results & Discussion

Macro- and Microstructural Analysis

Macrostructural insights.

Macrostructural images of T-joint specimens prepared with Al and Ti as skin and stringer alternatively are displayed in Fig. 4 and Fig. 5. The macrostructure was characterized by very distinctive featured flow arms of different materials and dimensions. These arms are generated by distinctive material flow patterns recorded with varied slot sizes and welding conditions. The size of the flow arm greatly influences the resulting properties owing to the skin/stringer material interlocking. During FSW of T-joints, as soon as the rotating tool pin penetrates the stringer material, it pushes the material underneath the tool to get extruded in the opposite direction, being constrained by the surrounding skin material. Simultaneously, the skin material flows downwards to the sides of the stringer material. As a result, engendered flow arms can be noticed in the vicinity of the thermo-mechanically affected zone (TMAZ) area as schematically represented in Fig.s 6 (a) and (b). Chen et al [13] have reported and corroborated the matching phenomenon of "extruded hook" during the FSW of Al-Ti lap joint configurations. The specific thermal contribution (STC) ensuing from distinct RP majorly contributes to the size of this flow arm, too.

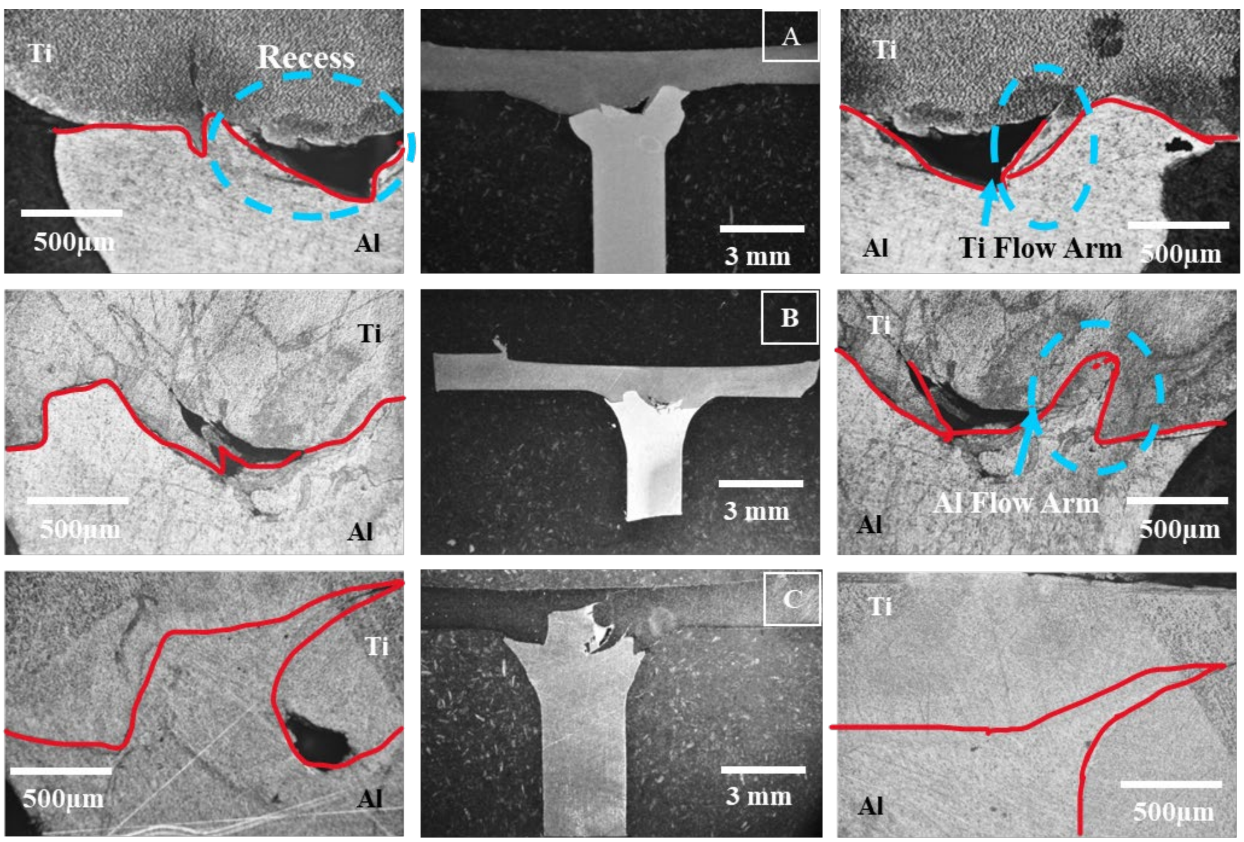

Fig. 4. Macrostructures of Ti skin Al stringer T-joints prepared with the skin-slot depth of (A) 0 mm (B) 0.5 mm (C) 1 mm.

As indicated earlier in the introduction section, FSW parameters were finalized using the author's previous publication. Ti skin/Al stringer samples were prepared with TRS and TTS of 400 rev. min^{-1} and 40 mm min^{-1}. However, the microstructure of this sample was characterized by a recess defect in the NZ. Such defects incurred owing to a huge property mismatch between skin and stringer materials, making it extremely challenging to get a synchronized material in the NZ. The flow stress at room temperature for Al is ¼ of the Ti, making Al soften in the advanced stage of the FSW stirring, while Ti resists the deformation. Although such mismatch can be minimized at elevated temperatures with a low RP value parametric set, it is not possible to eradicate. Hence, to minimize the flow resistance of the Ti skin material a novel strategy proposing a longitudinal slot in the skin was experimented as schematically exhibited in Fig. 6(c). Therefrom, the samples with 2 longitudinal slots with depths of 0.5 mm and 1 mm were milled prior to the FSW. The slot width was kept equal to the stringer plate thickness. It was believed that the slot shall not only reduce the volume of the Ti material to be deformed and stirred but increase the flow arm size as indicated schematically in Fig. 6(c). The micrographs of the Ti skin samples welded with the 0.5 mm and 1 mm slot depth are displayed in Fig. 4(B) and (C) respectively. As the proposed strategy, the tool pin not only minimized the recess defect size in NZ up to a great extent but allowed the Al flow arm to penetrate the Ti skin material. Still, it was not possible to omit the recess/pocket in the NZ completely. Moreover, the small Ti flow arms engendered by tool-driven extrusion were also identified in these samples indicating the greater softening of the Ti skin. The flow arm interlocking was also visible in these samples.

Nevertheless, the material flow that happened in the Al skin samples was quite different than in Ti skin and it was possible to extract a few defect-free samples at different processing conditions. As far as the Al skin samples are concerned, these samples were characterized by the longer Ti flow arm penetrating the Al skin as displayed in Fig. 5. As discussed in the preceding work, with a decrease and increase in the RP and STC values respectively the flow arm length was reportedly increased delivering the best joint strength. Therefrom, to further increase the flow arm size, a slot design was proposed. As the proposed strategy, the Ti flow arm size was drastically increased with the greater tool-driven extrusion. However, at the same time the larger extent of the extrusion created a larger void to fill in between two Ti flow arms ensuing into the recess/pocket in each sample prepared with slot (see Fig. 5 (E), (F), (H) and (I)). As mentioned earlier, the profile of this stringer arm is quite important for an interlocking mechanism during the T-pull test. It was observed that, while on one hand its vertical alignment (perpendicular to the skin), creates the least disturbance to material momentum while stirring, on the other hand, the horizontal alignment barricades the material flow toward the center and results in recess/pocket defects[9]. It is worth noticing that the flow arm length grows in the vertical direction with slot depth, but once it crosses a threshold value it starts bending towards the center of the weld as schematically represented in Fig. 7. This can be explained as when the slot depth is increased the shoulder rotates closer to the extruded stringer arm, engendering tremendous pressure on the stirring material, which bends the flow arm in the plane parallel to the shoulder face as visible in specimens F and I. This Ti flow arm boundary barricades the skin material to flow toward the center of NZ leaving back unfilled voids. Hence, as far as the slot depth is concerned the joints prepared with 0.5 mm slot exhibited longer and vertically aligned flow arms compared to others.

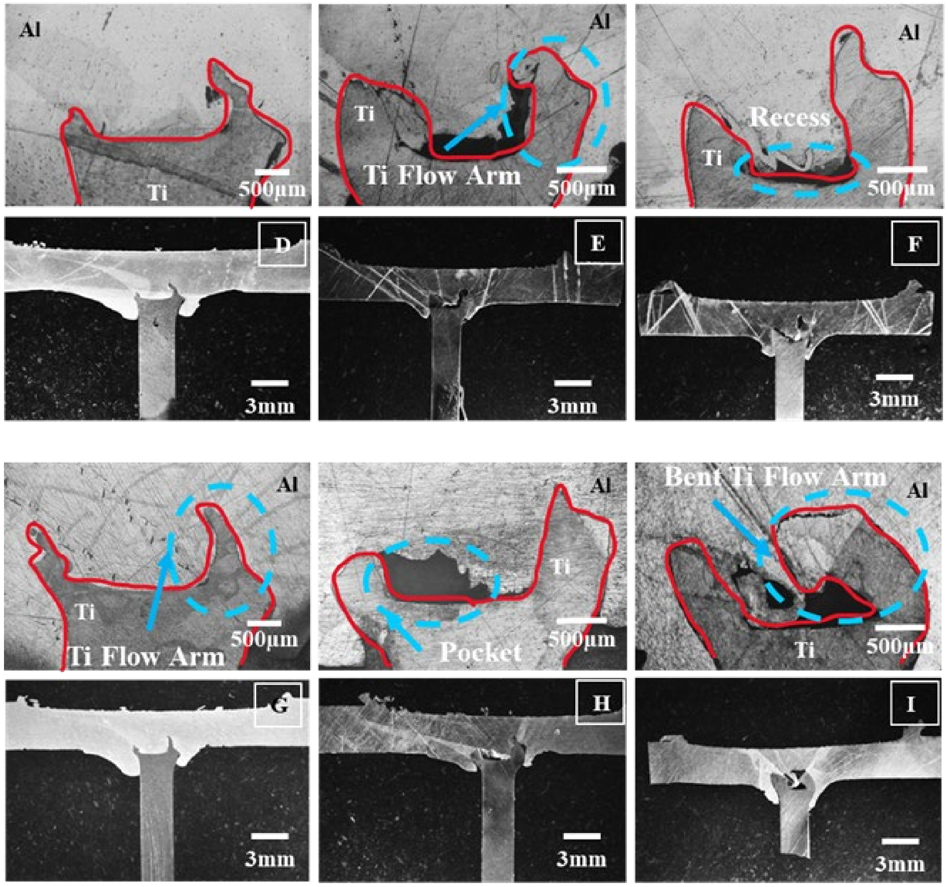

Fig. 5. Macrostructures of Al skin Ti stringer T-joints prepared with slot depth, TRS, and TTS of (D) 0 mm, 800 rev. min^{-1},50 mm min^{-1} (E) 0.5 mm, 800 rev. min^{-1},50 mm min^{-1} (F) 1 mm, 800 rev. min^{-1},50 mm min^{-1} (D) 0 mm, 1000 rev. min^{-1}, 70 mm min^{-1} (E) 0.5 mm, 1000 rev. min^{-1}, 70 mm min^{-1} (F) 1 mm, 1000 rev. min^{-1}, 70 mm min^{-1}.

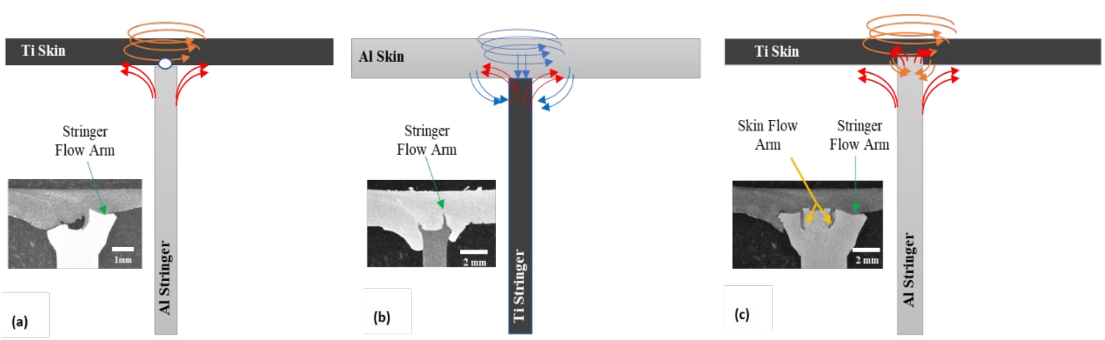

Fig. 6. Schematic exhibits for proposed material flow phenomenon in (a) Ti skin Al stringer (b) Al skin Ti stringer (c) proposed Ti skin with slot Al stringer.

Apart, defects like skin thinning and kissing bonds were also observed in the few samples (viz., B, C, H, I). Kissing bonds are reportedly formed either when the substrate materials are extremely asymmetric or they are inadequately heated and stirred. This eventually promotes the formation of residual oxide layers (e.g. TiO_2 in the present investigation) detached from the other substrate [14]. These layers wane the material attachment and raise the localized stresses during weld solidification. Especially for T-joint configuration, as the tool pin rotation plane is parallel to the joint interface, it becomes difficult to slash these oxide layers [12].

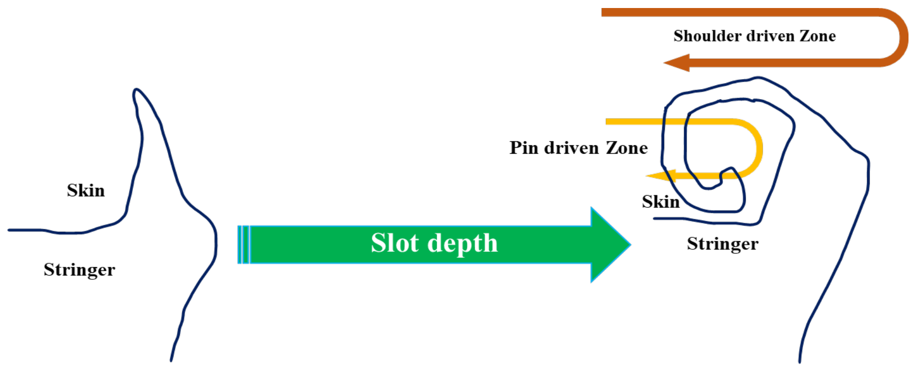

Fig. 7. Schematic representation of change in stringer flow arm profile concerning slot depth.

Microstructural insights.

The SEM and EDS mapping were carried out for the samples with no skin slot and maximum slot depth viz., G and F respectively. The mapping indicated the composite structure near the extruded Ti flow arm for both samples as displayed in Fig. 8. During FSW, when the extruded Ti stringer flow arm reaches the threshold length value, it starts interacting with the rotating shoulder. Further, the Ti flow arm experiences grinding led by the shoulder, leaving fine Ti particles in the vicinity of the flow arm. Rostami et al.[7] have reported the identical occurrence of the composite structure close to the Ti hook profile generated during FSW of Al-Ti lap joints.

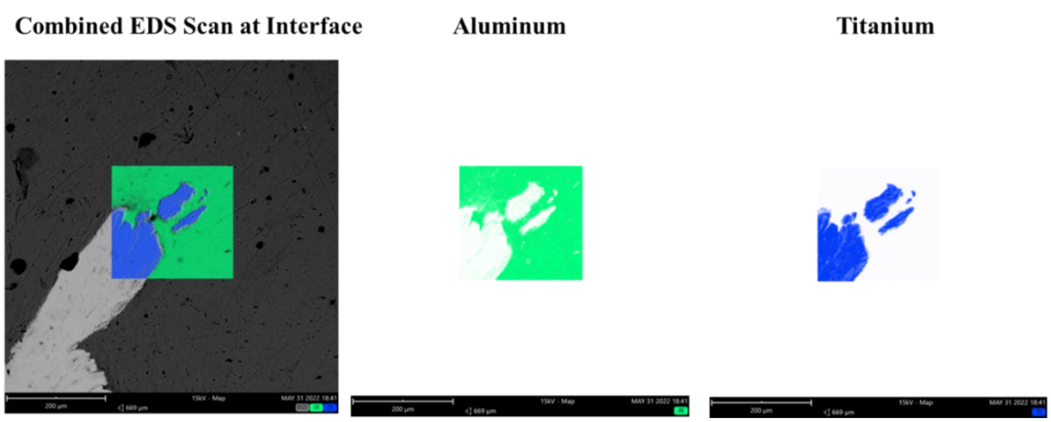

Fig. 8. SEM-EDS mapping of the composite structure near the Ti Flow Arm.

Moreover, the obtained results during the SEM-EDS analysis indicated a very thin and intermittent layer of $TiAl_3$ intermetallic close to the Al-Ti interface as exhibited in Fig. 9. It is noteworthy that the IMC layer thickness ranged from ~ 1 µm to 5 µm, which may be believed to be very lean considering the observed thickness for FSW butt and lap configuration joints [10, 13]. However, a thicker IMC layer was identified in the vicinity of the extruded Ti flow arm. This variable layer thickness at different locations may be understood by the successive events taking place while FSW. On the one side, when the rotating plunges adjacent to the Al-Ti interface, owing to softening of the Al skin led by high frictional heat, the Ti face is pressed downward and extruded as a flow arm leaving an unfilled void. This void remains empty until the tool progress along the joint line and stirring Al enters at the back of the tool.

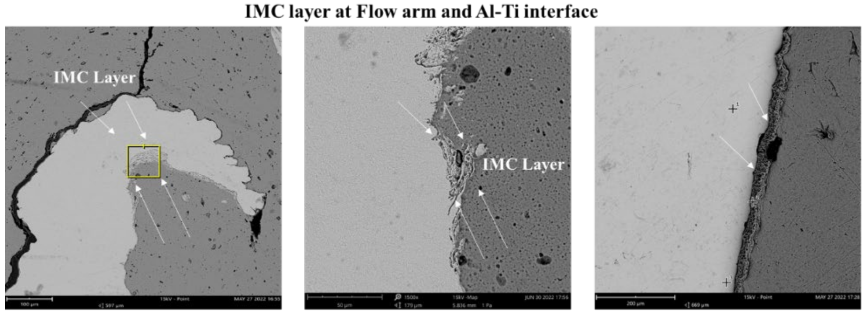

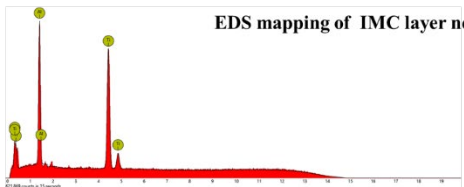

Element Symbol	Atomic Conc.	Weight Conc.	Oxide Symbol	Stoich. Wt.% Conc.
Al	69.11	55.78	Al_2O_3	58.83
Ti	30.89	44.22	TiO_2	41.17

Fig. 9. SEM/EDS mapping of Intermetallic Layer at Al-Ti interface and near the extruded Ti flow arm.

However, by the time Al fills the void completely, the temperatures of both Al and Ti are slightly dropped to a level at which the occurrence of Al-Ti diffusion is very minimal. While of the other side, when the extruded Ti flow arm penetrates Al, the temperatures of both substrates are elevated, leading to the Al-Ti diffusion and formation of a thick layer of IMC. The prevalent IMC phase identified in the NZ was $TiAl_3$. The mechanical properties of the prepared FSW joints are greatly influenced by the location, size, and amount of such IMCs.

Mechanical Properties

The joint strengths observed with T-pull test of all the samples are graphically displayed in Fig. 10. Concerning Ti skin samples, they were characterized by a moderate joint strength, which can be attributed to defects like porosity, recess, etc., and lack of appropriate flow arm interlocking phenomenon. Although the slots allowed the Al flow arm to enter into the Ti skin, there was a lack of proper interlocking. Still, a slight improvement in the joint strength can be observed for the samples prepared with the skin slots. While concerning the Al skin samples, the highest joint strengths of 146 MPa and 144 MPa were observed for sample G and sample D, respectively which were prepared without any skin slot. Although T-joints created with skin slots demonstrated longer extruded flow arms, they were characterized by recess and unfilled cavity defects as described earlier in section 3.1. Alternatively, quite comparable strength of 107 MPa was recorded with the sample I which was prepared with 1 mm slot depth. While comparing the performance of the slot depth in terms of joint strength, the deeper skin slot of 1 mm exhibited considerably superior results which can be attributed to the longer flow arm accompanied by the superior flow arm interlocking with skin in the NZ.

As far as the hardness results are concerned, the substrate materials Ti grade 2 and AA 6156 exhibited a hardness of 115 HV and 40 HV respectively. The hardness values recorded in the NZ of sample G were almost 50 % higher than the unprocessed substrate. The increased hardness values can be attributed to the Al-Ti composite structure, grain refinement, and IMCs present in the NZ of the welded samples [3,15,16]. Such rise in the hardness values can be backed by several strengthening mechanisms viz., shear lag mechanism and dislocation strengthening mechanism. According to the shear lag mechanism, as NZ is characterized by Ti particulate composite structure, during testing when the specimen is loaded the load is transferred from the Al matrix to very hard Ti particulates. The shear stress is generated at the Al-Ti interface due to this load shift, which eventually hinders the dislocation motion and ensures higher properties. As per dislocation strengthening, owing to a large mismatch of coefficient of thermal expansion between two substrates, geometrically indispensable dislocations are engendered at the Al/Ti interface and in the vicinity to the Ti particulates and IMCs, during the cooling period post-thermos-plastic deformation led by FSW. These dislocations impede crack growth and thereby increase joint strength and hardness. In the nutshell, the T-joints prepared with FSW not only exhibited the metallurgical bonding but the mechanically interlocked bonding too which promises an effective approach for the production of dissimilar material T-joints.

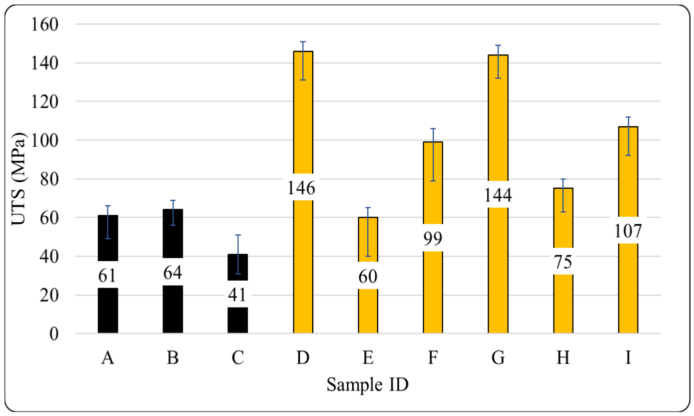

Fig. 10. Joint strength for Ti and Al skin samples.

Summary

This novel investigation describes the successful fabrication of dissimilar T-joints using Ti Gr 2 and AA6156 substrates, wherein the effects of mutual sheet position and innovative skin slot design on macrostructural, microstructural, and mechanical properties of the joints have been discussed in depth. The obtained conclusions are as under:

- AA 6156 substrate skin samples displayed substantially better properties than Ti substrate skin samples.
- The dissimilar material T-joint was characterized by interesting material flow patterns. Particularly, the development and geometry of the extruded flow arm were found to be crucial for mechanical interlocking resulting in improved joint strength. The length of this flow arm is directly proportional to the amount of heat input during the process and skin-slot depth. However, too large values of any of them can bend the flow arm which hinders the appropriate material flow leaving behind defects like cavities, recess, etc, and eventually reducing the mechanical properties.
- The samples produced without skin-slot exhibited superior joint strength as compared to skin-slot samples, owing to the formation of the defects like cavities and recesses in skin-slot samples. However, samples joined with a maximum slot depth of 1 mm exhibited superior joint strength as compared to 0.5 mm slot depth, owing to better mechanical interlocking of the flow arm with Al skin substrate.
- The hardness values of prepared T-joints were improved by 50% and 20% as compared to the unprocessed Al skin substrate and Ti stringer. Such an increase can be attributed to the Ti-particulate composite structure, grain refinement, and IMCs-led strengthening mechanisms.

References

[1] W. Vaidya, M. Horstmann, V. Ventzke, B. Petrovski, M. Koçak, R. Kocik, G. Tempus, Improving interfacial properties of a laser beam welded dissimilar joint of aluminium AA6056 and titanium Ti6Al4V for aeronautical applications, J. Mater. Sci. 45 (2010) 6242-6254. https://doi.org/10.1007/s10853-010-4719-6

[2] W. Shouzheng, L. Yajiang, W. Juan, L. Kun, Research on cracking initiation and propagation near Ti/Al interface during TIG welding of titanium to aluminum, Kovove Mater. 52 (2014) 85-91. http://doi.org/10.4149/km2014285
[3] P. Patel, H. Rana, V. Badheka, V. Patel, W. Li, Effect of active heating and cooling on microstructure and mechanical properties of friction stir–welded dissimilar aluminium alloy and titanium butt joints, Weld World 64 (2020) 365-378. https://doi.org/10.1007/s40194-019-00838-6
[4] Y.-C. Kim, A. Fuji, Factors dominating joint characteristics in Ti–Al friction welds, Sci. Technol. Weld. Join. 7 (2002) 149-154.
[5] L. Fratini, G. Buffa, L.L. Monaco, Improved FE model for simulation of friction stir welding of different materials, Sci. Technol. Weld. Join. 15(3) (2010) 199-207.
[6] A. Simar, M.-N. Avettand-Fènoël, State of the art about dissimilar metal friction stir welding, Sci. Technol. Weld. Join. 22(5) (2017) 389-403. https://doi.org/10.1080/13621718.2016.1251712
[7] H. Rostami, S. Nourouzi, H.J. Aval, Analysis of welding parameters effects on microstructural and mechanical properties of Ti6Al4V and AA5052 dissimilar joint, J. Mech. Sci 32 (2018) 3371-3377. https://doi.org/10.1007/s12206-018-0640-8
[8] B. Li, Z. Zhang, Y. Shen, W. Hu, L. Luo, Dissimilar friction stir welding of Ti–6Al–4V alloy and aluminum alloy employing a modified butt joint configuration: Influences of process variables on the weld interfaces and tensile properties, Mater. Des 53 (2014) 838-848. http://doi.org/10.1016/j.matdes.2013.07.019
[9] A. Kar, S. Suwas, S.V. Kailas, Multi-length scale characterization of microstructure evolution and its consequence on mechanical properties in dissimilar friction stir welding of titanium to aluminum, Metall. Mater. Trans. A 50 (2019) 5153-5173.
[10] Z. Ma, X. Sun, S. Ji, Y. Wang, Y. Yue, Influences of ultrasonic on friction stir welding of Al/Ti dissimilar alloys under different welding conditions, Int. J. Adv. Manuf. Technol. 112 (2021) 2573-2582. https://doi.org/10.1007/s00170-020-06481-6
[11] A. Kar, S.K. Choudhury, S. Suwas, S.V. Kailas, Effect of niobium interlayer in dissimilar friction stir welding of aluminum to titanium, Mater. Charact. 145 (2018) 402-412. http://doi.org/10.1016/j.matchar.2018.09.007
[12] H. Rana, D. Campanella, G. Buffa, L. Fratini, Dissimilar titanium-aluminum skin-stringer joints by FSW: process mechanics and performance, Mater. Manuf. Process. 38 (2023) 471-484. https://doi.org/10.1080/10426914.2022.2116044
[13] Y. Chen, C. Liu, G. Liu, Study on the joining of titanium and aluminum dissimilar alloys by friction stir welding, Open Mater. Sci. 5 (2011). http://doi.org/10.2174/1874088X01105010256
[14] Y. Su, W. Li, F. Gao, A. Vairis, Effect of FSW process on anisotropic of titanium alloy T-joint, Mater. Manuf. Process. 37 (2022) 25-33. https://doi.org/10.1080/10426914.2021.1942911
[15] H. Rana, V. Badheka, A. Kumar, A. Satyaprasad, Strategical parametric investigation on manufacturing of Al–Mg–Zn–Cu alloy surface composites using FSP, Mater. Manuf. Process. 33 (2018) 534-545. https://doi.org/10.1080/10426914.2017.1364752
[16] E. Lertora, C. Mandolfino, C. Gambaro, Effect of welding parameters on AA8090 Al-Li alloy FSW T-joints, Key Eng. Mater. 554c(2013) 985-995. http://doi.org/10.4028/www.scientific.net/KEM.554-557.985